PHYSICAL REVIEW B VOLUME 28, NUMBER 11 1 DECEMBER 1983

Monte Carlo and renormalization-group studies of surface structural phase transitions

L. D. Roelofs
Physics Department, Brown University, Providence, Rhode Island 02912
*and Physics Department, Haverford College, Haverford, Pennsylvania 19041**

G. Y. Hu and S. C. Ying
Physics Department, Brown University, Providence, Rhode Island 02912
(Received 31 May 1983)

The ϕ^4 model for structural phase transitions in two dimensions is studied using the Migdal renormalization-group method and a Monte Carlo coarse-graining calculation. The methods employed are useful for more general models of surface reconstructive transitions. Particular emphasis is placed on accuracy of phase diagrams and the nature of the "crossover" from order to disorder behavior above (in temperature) but close to the phase transition and displacive behavior at higher temperatures. The Monte Carlo coarse-graining calculation is found to give the fullest information on this crossover and the short-range order above the transition and also verifies the accuracy of the more economical Migdal calculation of the phase diagram. The results are discussed with reference to the surface reconstruction phase transition of the clean W(001) surface.

I. INTRODUCTION

The study of surface phase transitions has attracted much attention recently. This is due to both the increasing availability of experimental data for adsorption systems[1] and the theoretical interest for ordering in two dimensions.[2] Most of these phase transition studies concern the different phases of adsorbates arising from adsorbate-adsorbate and adsorbate-substrate interactions. However, it has also been discovered that a large number of metal and semiconductor surfaces exhibit reversible phase transitions even in the absence of the adsorbates.[1-9] These transitions are usually from a high-symmetry structure to one of lower symmetry as the temperature is lowered. This is the case, for example, on the (001) surface of W where the transition is from a (1×1), i.e., the two-dimensional (2D) symmetry of the bulk termination, to a $c(2\times2)$ structure occuring somewhat below room temperature.[3,10,11] The lower-symmetry phase can also be incommensurate with the underlying bulk layers as exemplified by the low-temperature phase of Mo(001).[3] Occasionally a whole sequence of transitions between different structures can take place as the temperature and/or coverage is varied.[3] All these diverse intrinsic surface phase transitions are truly 2D in character, since experimental studies have confirmed that only atoms in the first few layers are displaced from their bulk positions.[12,13] This is in contrast to the layer compounds where because of interlayer coupling, the character of the phase transition sufficiently close to the transition temperature is still three dimensional (3D).[14] From a theoretical point of view, this rich variety of 2D structural phase transitions provides an exciting test for various concepts.

Prior to the observation of surface structural phase transitions, bulk structural transitions in the ferroelectric compounds of the perovskite family such as $SrTiO_3$ (Refs. 15 and 16) and $LaAlO_3$ (Ref. 17) had been extensively studied. A key question in these studies concerned the distinction between the "displacive" and "order-disorder" character of the phase transition.[15-21] In the displacive regime the transition is thought to occur via gradual displacement of groups of atoms from their high-temperature equilibrium positions as the temperature is lowered. This is often described as the condensation of a soft mode whose frequency goes to zero at the transition point.[21] By contrast a transition of order-disorder character occurs when groups of atoms have several equivalent (usually displaced relative to the bulklike positions) sites and a long-range correlation in the occupation of these sites develops at the transition in a manner analogous to transitions in spin systems.[21,22] The modern theory of structural phase transitions unifies these two points of view, and it is now recognized that even in a displacive system, clusters of atoms will develop an order-disorder character, and that the conventional soft-mode picture is inadequate for describing the dynamics and the short-range order.[21(b)] The validity of this new concept depends crucially on the dimensionality of the system. In three dimensions, theoretical and experimental evidence for a cluster picture are not pronounced.[21(c)] However, according to existing theories, the cluster character should be more evident in lower-dimensional systems.[21(b)] Thus the actual realization of experimental systems is extremely important for establishing the new unified view of structural phase transitions. In this paper we present a Monte Carlo and renormalization-group study of a model Hamiltonian that contains the essential features of a 2D structural phase transition. Particular emphasis will be made on the development of short-range order just above T_c and the crossover from order-disorder to displacive behavior at higher temperature. We then review the experimental data for W(001) and argue that this provides

qualitative support of the theoretical cluster picture near T_c that emerges from our study.

II. MODEL HAMILTONIAN

A standard model Hamiltonian that contains the essential features of structural phase transitions is given by[21(a),23]

$$H=T(\{\vec{p}_{\vec{l}}\})+V(\{\vec{u}_{\vec{l}}\}) , \tag{2.1a}$$

where

$$T=\frac{1}{2m}\sum_{\vec{l}}\vec{p}^{\,2}_{\vec{l}} , \tag{2.1b}$$

$$V=\sum_{\vec{l}}V_s(\vec{u}_{\vec{l}})+\frac{C}{2}\sum_{\vec{l},\vec{l}'}^{\mathrm{NN}}(\vec{u}_{\vec{l}}-\vec{u}_{\vec{l}'})^2 . \tag{2.1c}$$

Here, $\vec{u}_{\vec{l}}$ and $\vec{p}_{\vec{l}}$ describe, respectively, the displacements and momenta of a set of atoms whose high-temperature phase equilibrium positions occupy a square lattice $\{\vec{l}\}$. The on-site potential V_s has double-well character. In the usual 3D study of this model Hamiltonian, V_s is thought of as arising from a sublattice of "inert" atoms which do not participate actively in the phase transition. In the case of surfaces, if $\vec{u}_{\vec{l}}$ and $\vec{p}_{\vec{l}}$ refer to the surface layer atom coordinates only, then V_s arises naturally from the underlying layers of atoms. Of course a simple Hamiltonian as given in (2.1a)—(2.1c) is not sufficient for describing the incommensurate phases or more complicated superlattice structures with large unit cells. It is, however, appropriate for describing the most studied surface structural transition on W(001) with two qualifications. First, since the transition on clean W(001) is from a 1×1 to $c(2\times2)$ structure, the actual displacement of an individual surface atom is not $\vec{u}$ but

$$\hat{\vec{u}}_{\vec{l}}=\vec{u}_{\vec{l}}\cos(\vec{k}\cdot\vec{l}) , \tag{2.2}$$

with $\vec{k}=(\pi/a,\pi/a)$; a is the lattice constant.

The phase factor $\cos(\vec{k}\cdot\vec{l})$ provides an alternating sign on adjacent sites that converts a uniform displacement $\vec{u}$ into one appropriate for a $c(2\times2)$ structure. This is analogous to the relation between the ferromagnetic and antiferromagnetic states.[24] Second, detailed low-energy electron diffraction (LEED) intensity analyses[12,13] have shown that the transitions occuring on W(001) involves the in-plane motion of surface atoms (see, however, Refs. 25—27). Thus the displacement vector $\vec{u}_{\vec{l}}$ in (2.1c) is properly a two-component vector. However, in this paper we shall restrict ourselves to a single-component scalar displacement $u_{\vec{l}}$. This simplifies the calculations allowing better understanding of the qualitative features which should carry over into the two-component situation also. We have also undertaken calculations on the two-component model. These will be discussed in a forthcoming paper.[28]

It is interesting to note that in the presence of a strong electric field, such as that employed in a field ion desorption experiment, the structural phase transition on W(001) may be better described by a vertical scalar displacement rather than an in-plane movement.[25—27] Thus the study of a scalar model is of more than qualitative interest. In keeping with the bulk of the literature, we shall take the potential V_s to be the simplest one displaying a double-well character,

$$V_s=-\tfrac{1}{2}Au^2+\tfrac{1}{4}Bu^4 . \tag{2.3}$$

This simplification is not actually necessary in our calculation but it does facilitate the comparisons between our results and existing work in the literature. For $A>0$, V_s has a pair of minima at $u_0=\pm(A/B)^{1/2}$. Of particular interest is the dimensionless quantity,

$$s=-\frac{V_s(u_o)}{2Cu_0^2}=-\frac{A}{8C} . \tag{2.4}$$

This is just the ratio of well depth to the bond energy associated with moving one particle from the top to the bottom of the well. The limit $s\gg1$ represents the order-disorder limit, while for $s\ll1$, the thermal energy at T_c is large in comparison to the well depth $V_s(u_0)$, corresponding to the displacive limit.

We shall study the Hamiltonian only in the classical regime. For evaluation of the configuration partition function, it is convenient to consider an effective Hamiltonian $\mathscr{H}=-\beta V$. Also, following Beale, Sarker, and Krumhansl (BSK),[23] we can eliminate one of the parameters by rescaling the field variable,

$$u_{\vec{l}}\rightarrow u'_{\vec{l}}=\zeta u_{\vec{l}} . \tag{2.5a}$$

Then

$$\mathscr{H}=\sum_{\vec{l}}\left[\frac{K}{2}\theta u^2_{\vec{l}}-\frac{K(\theta+1)}{4}u^4_{\vec{l}}\right]-\sum_{\vec{l},\vec{l}'}^{\mathrm{NN}}\frac{K}{2}(u_{\vec{l}}-u_{\vec{l}'})^2 , \tag{2.5b}$$

with the dimensionless parameters,

$$K=\frac{\beta C^2}{B}(1+\theta) , \tag{2.5c}$$

$$\theta=\frac{A}{C} . \tag{2.5d}$$

K is the inverse temperature measured in appropriate units and θ, being proportional to s defined in (2.4), is a measure of the displaciveness of the Hamiltonian.

III. MIDGAL RENORMALIZATION TRANSFORMATION

In this section we present a Migdal renormalization-group calculation of the phase diagram of the model defined in the preceding section. We follow the approach of BSK, but our method differs from theirs in several important respects as do our results. The Monte Carlo simulations described in Sec. IV verify the validity of these improvements.

A. Transfer-matrix implementation of migdal approximation

The partition function may be written

$$Z = \mathrm{Tr}\exp(\mathscr{H}) , \tag{3.1a}$$

$$= \int_{-\infty}^{\infty} \left[\prod_{\vec{l}} du_{\vec{l}} \right] \exp[\mathscr{H}(\{u_{\vec{l}}\})] \tag{3.1b}$$

$$= \int_{-\infty}^{\infty} \left[\prod_{\vec{l}} du_{\vec{l}} \right] S(u_{\vec{l}_1},u_{\vec{l}_2}) S(u_{\vec{l}_2},u_{\vec{l}_3}) \cdots , \tag{3.1c}$$

where

$$S(u_{\vec{l}},u_{\vec{l}'}) = \exp\left[-\frac{K}{2}(u_{\vec{l}}-u_{\vec{l}'})^2 + \mathscr{V}(u_{\vec{l}},u_{\vec{l}'}) \right] , \tag{3.2a}$$

and $\mathscr{V}$ denotes the on-site part of the potential

$$\mathscr{V}(u_{\vec{l}},u_{\vec{l}'}) = \frac{1}{4}K\left[\frac{\theta}{2}(u_{\vec{l}}^2+u_{\vec{l}'}^2) - \frac{\theta+1}{4}(u_{\vec{l}}^4+u_{\vec{l}'}^4) \right] . \tag{3.2b}$$

The factor of $\frac{1}{4}$ derives from the fact that each site attaches to four bonds in the square lattice.

S as defined by (3.2) is just the transfer "matrix" (here in continuous form so that the appellation "transfer integrand" might be more apt), which can be used to solve classical models on one-dimensional (1D) lattices.[29] Since the essence of the Migdal approximation is to reduce the difficult decimation procedure to a 1D problem (usually by moving bonds),[30] the transfer-matrix formulation is convenient.

We associate a transfer matrix with each nearest-neighbor bond of the lattice, denoting horizontal bonds by S_x and vertical bonds by S_y. The standard Migdal approximation for a square lattice (see Fig. 1) involves first moving half the horizontal bonds one lattice spacing in the vertical direction. This doubles the strength of the remaining horizontal bonds so that

$$S_x'(u_{\vec{l}},u_{\vec{l}'}) = [S_x(u_{\vec{l}},u_{\vec{l}'})]^2 . \tag{3.3}$$

Meanwhile, the sites which connect only to vertical bonds can now be decimated giving a renormalized interaction in the vertical direction,

$$S_y'(u_{\vec{l}},u_{\vec{l}'}) = \int_{-\infty}^{\infty} du_{\vec{l}''} S_y(u_{\vec{l}},u_{\vec{l}''}) S_y(u_{\vec{l}''},u_{\vec{l}'}) . \tag{3.4}$$

The process is then repeated with the directions interchanged,

$$S_y''(u_{\vec{l}},u_{\vec{l}'}) = [S_y'(u_{\vec{l}},u_{\vec{l}'})]^2 , \tag{3.5}$$

$$S_x''(u_{\vec{l}},u_{\vec{l}'}) = \int_{-\infty}^{\infty} du_{\vec{l}''} S_x'(u_{\vec{l}},u_{\vec{l}''}) S_x'(u_{\vec{l}''},u_{\vec{l}'}) , \tag{3.6}$$

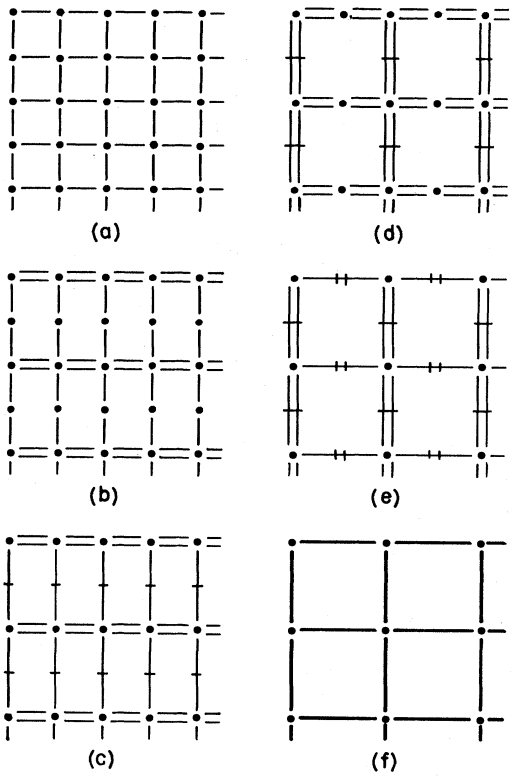

FIG. 1. Steps in the Migdal iteration. See text.

yielding a renormalized transfer matrix defined on a lattice whose spacing has increased by a factor of 2 in each direction, and whose number of sites has been reduced by a factor of 2^2.[31] Equations (3.3)—(3.6) result in unsymmetric transfer matrices ($S_x \neq S_y$). We therefore average the renormalized couplings,

$$S^{(2)}(u_{\vec{l}},u_{\vec{l}'}) = [S_x''(u_{\vec{l}},u_{\vec{l}'}) S_y''(u_{\vec{l}},u_{\vec{l}'})]^{1/2} . \tag{3.7}$$

$S^{(2)}$ is the once renormalized (by a scale factor of 2) transfer matrix. One can examine the effect of renormalization on the Hamiltonian by considering the logarithm of $S^{(2)}$. Numerical implementation of the iteration implied by Eqs. (3.3)—(3.7) will be discussed below; we turn now to our first divergence from the method employed by BSK.

After each renormalization of S, BSK suggest mapping the resultant renormalized Hamiltonian back onto the original functional form by adjusting the coupling constants K and θ. By contrast we have explored the consequences of iterating Eqs. (3.3)—(3.7) without mapping back onto the original Hamiltonian after each renormalization. This procedure avoids ambiguities associated with the fitting procedure used to determine renormalized values for K and θ, and by eschewing truncation of the Hamiltonian (i.e., disposal of higher-order terms in $u_{\vec{l}}$) should allow more accurate calculation of phase boundaries. As will be seen below, this modification in procedure does lead to significant qualitative and quantitative variance with BSK's results and good agreement with Monte Carlo simulations.

B. Numerical implementation

Like BSK we have found it convenient to perform the decimation integrals in Eq. (3.4) and (3.6) by using a Gaussian-type quadrature.[32] After transforming the integration to the interval $[-1,1]$ using the substitution,

$$z=\tanh u \ , \tag{3.8}$$

we use the standard Gaussian points and weights to turn the integral into a simple matrix product,[33]

$$S_{ij}=S(u_i,u_j)\left[\frac{w_i w_j}{(1-z_i^2)(1-z_j^2)}\right]^{1/2} , \tag{3.9a}$$

$$u_i=\tanh^{-1} z_i \ , \tag{3.9b}$$

where z_i and w_i are, respectively, the Gaussian points and weights for the integration range $[-1,1]$. Equation (3.4), for example, then becomes

$$S'_{y,ij}=\sum_k S_{y,ik}S_{y,kj} \ . \tag{3.10}$$

The bond strengthening step of Eqs. (3.3) and (3.5) is also conveniently handled in the matrix formulation just by squaring matrix elements and accounting for the weight factor,

$$S'_{x,ij}=(S_{x,ij})^2\left[\frac{(1-z_i^2)(1-z_j^2)}{w_i w_j}\right]^{1/2} , \tag{3.11}$$

so that the $b=2$ Migdal iteration reduces to alternately squaring matrices and their individual elements.

As mentioned above, there seems to be no particular justification for mapping renormalized Hamiltonians back onto the original functional form. Instead we allow the flow to occur in the space of all two-body continuous nearest-neighbor interactions allowed by symmetry. (Ultimately the space is restricted by the discretization of the transfer "integrand," but the error introduced thereby can be systematically studied and controlled by increasing the number of grid points.) The fixed points that occur in this space are the low-temperature Ising ($K\to\infty$, $\theta\to\infty$) point, the Ising fixed point ($K_c=0.44068\ldots$, $\theta\to\infty$), the high-temperature (Gaussian) point ($K\to 0$, θ arbitrary), and the fully unstable point at ($K=0$, $\theta=0$). To follow the general direction of the flows it is useful to associate effective values of K and θ with a given renormalized Hamiltonian on the basis of the lowest-order terms included. To establish such an association we begin with the Hamiltonian after $(n-1)$ iterations,

$$\mathscr{H}_{ij}^{(n)}=\ln\left[S_{ij}^{(n)}\left[\frac{(1-z_i)(1-z_j)}{w_i w_j}\right]^{1/2}\right] . \tag{3.12}$$

The diagonal elements specify the on-site part of the potential,

$$\mathscr{H}_{ii}^{(n)}=\mathscr{H}^{(n)}(u_{\vec{1}},u_{\vec{1}'})\,|_{u_{\vec{1}}=u_{\vec{1}'}=u_i} \tag{3.13a}$$

$$=\mathscr{V}^{(n)}(u_{\vec{1}},u_{\vec{1}'})\,|_{u_{\vec{1}}=u_{\vec{1}'}=u_i} \ . \tag{3.13b}$$

The purely bond part of the Hamiltonian is

$$\mathscr{H}^{(n)}(u_{\vec{1}},u_{\vec{1}'})-\mathscr{V}^{(n)}(u_{\vec{1}},u_{\vec{1}'}) \ ,$$

which to leading order should vary like $-\frac{1}{2}K(u_{\vec{1}}-u_{\vec{1}'})^2$. We thus associate $K_{\rm eff}$ with the curvature around

$$(u_{\vec{1}}-u_{\vec{1}'})=0.0, \quad u_{\vec{1}}=0 \ .$$

Thus we have

$$K_{\rm eff}^{(n)}=-\frac{\ln S^{(n)}(u_1,u_1)-\ln S^{(n)}(u_1,u_1)}{2u_1^2} \ , \tag{3.14}$$

where $u_1=\tanh^{-1} z_1$, and z_1 is the first Gaussian point to the right of 0. The on-site part of the potential is tracked by using the first two diagonal elements of the transfer matrix to determine effective values of the first two terms in the expansion of the on-site part [see Eq. (2.3)] $A_{\rm eff}^{(n)}$ and $B_{\rm eff}^{(n)}$. Although the on-site part does not retain the scaled functional form under renormalization, an approximate value for $\theta_{\rm eff}$ in terms of $K_{\rm eff}$ is

$$\theta_{\rm eff}=\frac{1}{2}\left[\frac{A_{\rm eff}^{(n)}+B_{\rm eff}^{(n)}}{K_{\rm eff}^{(n)}}-1\right] . \tag{3.15}$$

The flow of $K_{\rm eff}^{(n)},\theta_{\rm eff}^{(n)}$ although it does not fully specify the evolution of the Hamiltonian, allows detection of the behavior under renormalization.

C. Moving the on-site potential

We have so far treated the on-site part of the potential on the same footing as the bond part, i.e., a fraction ($\frac{1}{4}$ for a 2D square lattice) of each on-site potential is attached to the end of each bond and moved along with it. Thus a fraction α equals one-half of each on-site potential is moved away from the site before decimation. Emery and Swendsen[34] pointed out that within the framework of the Migdal approximation, there is no necessity for moving the on-site potentials at all. Thus one can consider α to be an arbitrary (with the range $[0,\frac{1}{2}]$) parameter. Accordingly the effects of varying α have been investigated for several models. We have found, for example, in a study of the X-Y model with cubic anisotropy[28,35] that while the choice of α does not substantially effect the accuracy of the phase diagram obtained, significant quantitative improvement of the values of the eigenvalues is realized with the choice $\alpha=0$. We therefore investigated the effect of varying α in the present calculation.

Implementation is straightforward in the transfer matrix formulation, but in this case the results seem to be rather insensitive in all respects save one to the choice of α. The one major difference which effects neither the phase diagram nor exponent estimates, is the shape of the iterated on-site potential. Whereas the choice $\alpha=\frac{1}{2}$ never produces unusual renormalized on-site potentials, the choice $\alpha=0$ often gives on-site potentials after many iterations with three "valleys" reminiscent of the free-energy functional near a first-order transition. The behavior is seen, however, only on approach to the high- and low-temperature fixed points, and thus does not appear to have any physical significance.

D. Results

One disturbing aspect of the calculation of BSK to us is the poor agreement with our subsequent Monte Carlo calculations. This may have been due in part to the semiqualitative nature of their "phase diagram." However, we have found that most of the discrepancy is real and in fact results from the practice of mapping the iterated Hamiltonian back onto the simple two-parameter form of Eq. (2.5b). Our phase diagram (for both $\alpha=0$ and $\alpha=\frac{1}{2}$), the Monte Carlo results to be described in the following section, and BSK's results are given in Fig. 2, using the scales of BSK. The choice $\alpha=\frac{1}{2}$ for the on-site convention seems to give more favorable agreement. Our results also show that the Migdal renormalization scheme can in fact give a very accurate account of the phase diagram if the flow is unrestricted for these continuous models. This point is important because the Migdal calculation requires very little computer time in comparison to the Monte Carlo work. Thus even though the Migdal calculation does not give unambiguous information concerning short-range order and the displacive—order-disorder dichotomy cannot be straightforwardly addressed (see next section), it is useful for rapid, quantitative determination of phase diagrams.

There is a second difference between our results and those of BSK. They described on the basis of the flow of their Migdal calculations, a crossover behavior in the high-temperature region between order-disorder and displacive behavior. We will discuss this point more fully in Sec. V, but we find that this crossover behavior is not real in any long-range sense. Instead the distinction between the two types of behavior depends on the size of the region studied (i.e., the number of renormalizations done)

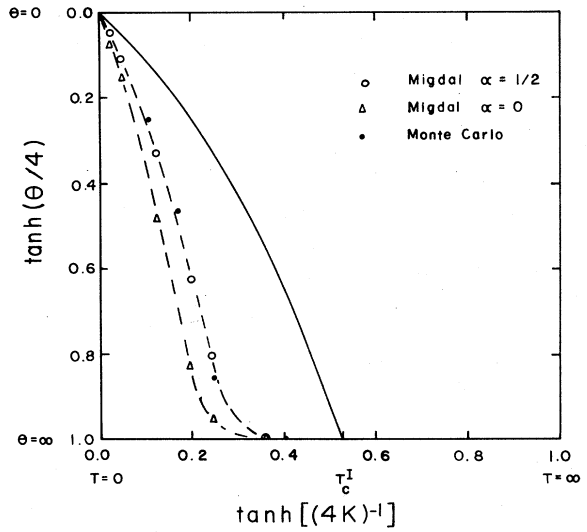

FIG. 2. Phase diagram of the θ^4 model. Solid line is the result of BSK (Ref. 23). Open circles and triangles are our Migdal renormalization group results with $\alpha=0$ and $\frac{1}{2}$, respectively. Filled circles are points obtained with Monte Carlo techniques (see Sec. IV). Dashed lines have no physical significance and are intended to guide the eye.

and it becomes less pronounced as K decreases. Thus there is no well-defined boundary between the behaviors as suggested by BSK. This boundary and the apparent fixed point terminating it are artifacts of the restriction on the Hamiltonian.

IV. MONTE CARLO CALCULATION

The Migdal renormalization scheme described in the preceding section provides a simple and fairly accurate way of analyzing phases associated with the Hamiltonian (2.5b). Our results in this section will also attest to this fact. The major drawback of the Migdal scheme for our present study is that it does not yield clear information about the short-range order just above the transition temperature. By restricting the renormalization flow in a two-parameter space, BSK produced a separatrix separating two regions in the (K,θ) space above T_c, one flowing towards the high-temperature Ising fixed point and the other towards the Gaussian point. (T_c denotes a critical transition temperature.) These two regions are then identified as having order-disorder character and displacive character, respectively. Although this division bears a qualitative relation to the presence or absence of short-range order or domains above T_c, the precise meaning of this separatrix is unclear in 2D. As shown in the preceding section, when one removes the restriction of the flow to a two-parameter space, the separatrix disappears altogether. Alternatively one can follow the *initial* flow in the parameter space to get a qualitative picture of the short-range order but again there is no way of mapping this information to the actual degree of short-range order above T_c. For these reasons, we have performed a Monte Carlo calculation on the model Hamiltonian (2.5b). The purpose of this study is twofold. The first is to check the accuracy of the Migdal scheme for the phase diagram, especially the relative merits of different ways of moving the on-site potential in the renormalization transformation. Second, the Monte Carlo results present a very clear picture of the short-range order above T_c and the cluster formation phenomena even in a "displacive system." The method we use is based on the Monte Carlo coarse-graining and renormalization scheme recently introduced by Binder[36] in a calculation for Ising spin systems. The idea is to examine the block order-parameter variable $u_L(\vec{l}\,')$ defined as

$$u_L(\vec{l}\,')=\frac{1}{L^2}\sum_{\vec{l}\in B(L,\vec{l}\,')} u_{\vec{l}}\ , \tag{4.1}$$

where $B(L,\vec{l}\,')$ represents the set of lattice sites in an $L\times L$ block centered at $\vec{l}\,'$. The Monte Carlo data are analyzed by studying the various moments

$$u_L^k=\int du\, u^k P_L(u)$$

of the block variable distribution function $P_L(u)$ for $k=2$, 4, 6, etc., and their lowest-order cumulants defined as

$$\begin{aligned} U_L&=1-\langle u_L^4\rangle/(3\langle u_L^2\rangle^2)\ , \\ V_L&=1-\frac{\langle u_L^4\rangle}{2\langle u_L^2\rangle^2}+\frac{\langle u_L^6\rangle}{30\langle u_L^2\rangle^3}\ . \end{aligned} \tag{4.2}$$

Above T_c, $P_L(u)$ becomes a Gaussian for $L \gg \xi$ (ξ being the correlation length, and hence U_L, V_L, ..., tend to zero as $L \to \infty$). Below T_c, $P_L(u)$ tends toward two delta functions centered at $\pm u_0$, the net displacement of each atom, and hence U_L, V_L approach the values $\frac{2}{3}$ and $\frac{8}{15}$, respectively. Right at T_c, Binder has argued that U_L approaches a nontrivial fixed value U^* as $L \to \infty$. (For $d=2$, $U^*=0.52$.) The great advantage of this method is that from one Monte Carlo run we obtain $P_L(u)$ for all L simultaneously up to the size of the system used in the calculation. Figure 3 shows the "flow" diagram for U_L based on Monte Carlo study of the Hamiltonian (2.5b) on a (24×24) lattice. The value of the parameter θ was taken to be 5.0 for this set of runs. About 3000 Monte Carlo steps per site are used. As can be seen from the figure, one can easily extract the value of $T_c=1.01\pm0.01$ from the extrapolation of U_L to large L. We have also tested numerically that to this accuracy, larger lattice size and longer runs produce no appreciable change of the transition temperature. Besides the transition temperature, the various block variable distributions provide a wealth of information about the short-range order. In Fig. 4, we have plotted the distribution $P_2(u)$ at various temperatures. At a temperature slightly above T_c, the correlation length ξ is still considerably longer than L times the lattice constant, and hence $P_L(u)$ maintains a double-peak character signaling the presence of short-range order or clusters of size larger than L. As one moves away towards higher temperature, eventually the correlation length becomes less than the size of the block. At this point, the block variable U_L is distributed around zero and $P_L(u)$ shows a single centered peak. This is a simple but accurate way of determining the variation of the correlation length above

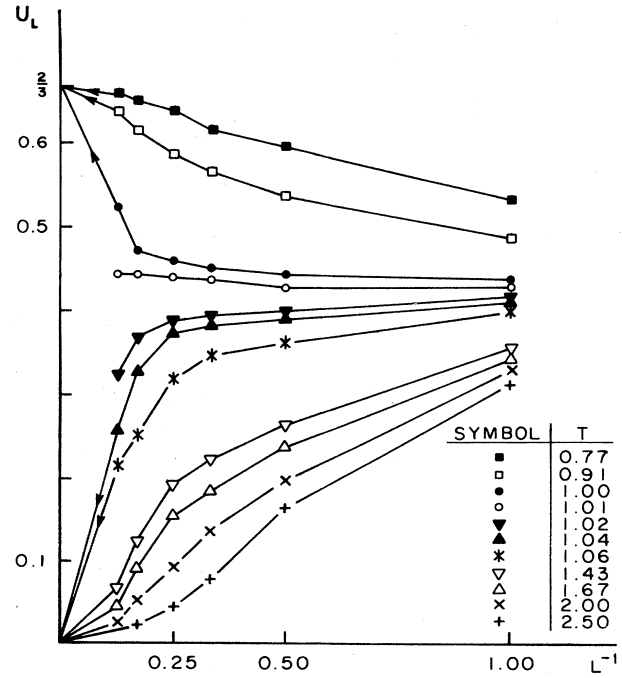

FIG. 3. Cumulant of block distribution function as a function of block size in a 24×24 lattice with $\theta=5.0$.

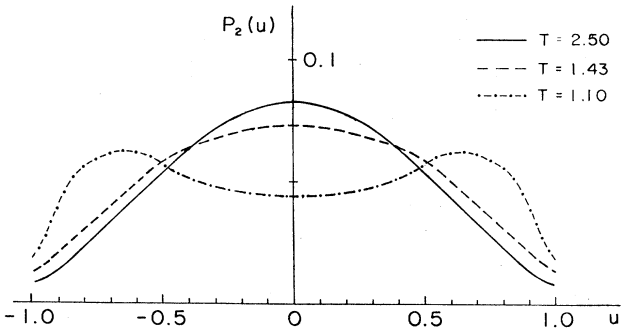

FIG. 4. Distribution for 2×2 block for temperatures well above (solid line), somewhat above (dashed curve), and slightly above (dotted-dashed curve) the critical temperature ($T_c=1.01$). Double-peaked character at $T=1.10$ shows the persistance of short-range order above T_c.

the transition temperature and the presence or absence of short-range order domains. Since U_L starts to decrease significantly towards zero only when L exceeds ξ, an even simpler way of deciding the transition between two regions is to set U_L to a certain value. Here, we have found by comparison with the behavior of $P_L(u)$ that a good choice for a "crossover" temperature $T_L(\theta)$ is the condition,

$$U_L[T_L(\theta),\theta]=0.2\ . \tag{4.3}$$

Note that if the block distribution $P_L(u)$ were a superposition of two Gaussians, the transition from single peak to double peak would occur at $U_L=\frac{1}{6}$.

With this criterion, one can now define a whole series of crossover boundaries, one for each L, besides the true phase boundary. For $T_c(\theta)<T<T_L(\theta)$, no long-range order exists but there are clusters of size larger than L. Thus the boundary $T=T_L(\theta)$ in the (T,θ) plane separates a high-temperature region with displacive character and a low-temperature region just above $T_c(\theta)$ with order-disorder character. In Fig. 5, we present the result for the phase diagram together with the $L=2$ and crossover boundaries. It is clear that even for $\theta \ll 1$, the region just above T_c always has an order-disorder character as also indicated by previous molecular dynamics[37] and renormalization-group studies.[38] Another point to note is that the true phase boundary can be viewed as the limiting curve for a sequence of crossover boundaries $T_L(\theta)$ in the limit $L\to\infty$, corresponding to the fact that the correlation length diverges at the transition temperature T_c. We note finally that the phase boundary obtained by the Migdal transformation (especially with $\alpha=\frac{1}{2}$) compares favorably with the Monte Carlo results.

V. DISCUSSION

In the preceding sections we have presented both the Migdal transformation and Monte Carlo results for a simple model Hamiltonian. The Migdal transformation provides an easy way of determining the phase diagram. It is, however, difficult to extract details of the short-range order from the results. Also, for a more realistic Hamiltoni-

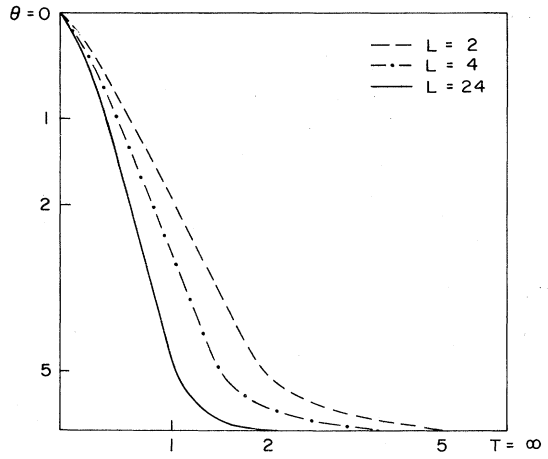

FIG. 5. Crossover boundaries for various block sizes in the ϕ^4 model. Scale is the same as that used in Fig. 2. Boundary corresponding to infinite L is the *phase* boundary; in Fig. 2 the phase boundary is taken to be the $L=24$ crossover boundary.

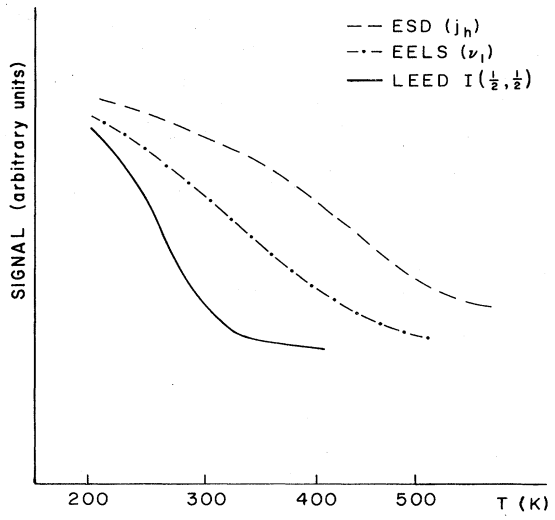

FIG. 6. Schematic sketches from data obtained in different types of experiments on the surface reconstruction phase transition of W(100) which measure the degree of order at different length scales (see text).

an appropriate for the description of surface structural phase transition, more than just nearest-neighbor interactions would be involved, and it is difficult to generalize the Migdal transformation to this situation. On the other hand, the Monte Carlo coarse-graining analysis of the block distribution function can be applied to more complicated Hamiltonians. In the presence of a small amount of adsorbates such as in the case of hydrogen on W(001),[39] we have shown that the absorbate degree of freedom can be integrated out and the resultant effective Hamiltonian would still be of the form presented in (2.1), with a potential energy $V(\{u_{\vec{l}}\};T,n)$ depending on both the temperature and fractional coverage n of the surface.[35] Thus by mapping the model calculation described in this paper to the effective Hamiltonian, we can study the phase diagram in the temperature-coverage (T,n) plane. This can be readily measured experimentally, and data for many adsorption systems are available for comparison with the theory.[1]

The Monte Carlo coarse-graining method also provides an easy analysis of the block variable distribution function $P_L(u)$ and the clustering phenomena above the transition temperature. Experimentally there is a set of data on W(001) that are relevant to this question. In Fig. 6, we have sketched schematically how three different quantities from different experiments on W(001) develop as a function of temperature. The first quantity is the intensity of the half-order spot in LEED data taken from Refs. 10 and 40. This is a measure of the (long-range) order parameter, i.e., the average displacement of the surface atoms. (Actually, LEED is limited to a coherence length of 100—300 Å.) The next curve refers to a local vibrational mode (ν_1) of hydrogen absorbed on the W(001) surface taken from Ref. 41. This mode is sensitive to the bond angle between H and W and hence to the *local* displacements of the W atom. Finally the last curve refers to the ionic current yield in an electron impact desorption experiment of H from W(001) from Ref. 42. Again the strong variation of this yield as a function of the temperature can be interpreted as an implication that the desorption yield is a sensitive function of the surface atom displacements. It is interesting to note the similarity between these sets of curves and the theoretical results in Fig. 5 for crossover at different values of the coherence length. This can be interpreted as evidence that the three different types of experiments, LEED, inelastic electron scattering spectroscopy (measurements of local vibrational modes), and electron impact desorption, are probing different ranges of order with regard to the structural phase transition on W(001); the LEED experiment probing the longest range and the desorption experiment probing the shortest. There are also other experimental data such as high-energy ion scattering[43] which obviously probe very-short-range order that fits into this description. One should bear in mind that the actual order parameter for W(001) transition has two components whereas the present study is for a scalar parameter. Nonetheless, we believe that the qualitative features presented here should carry over. Calculations for the two-component order parameter are underway and will be reported elsewhere.[28] Quantitative comparison of the theory with the experimental data is not warranted until better theories for the dependence of surface vibrational modes and electron impact desorption yield on the surface structure are available.

Finally we should mention that the original motivation for considering the cluster picture in the study of 3D structural phase transitions is the appearance of a central peak in the dynamic structure factor data for $SrTiO_3$.[15,16] This is currently understood as arising from the slow motion of domain walls as opposed to the other time scale set by the soft-mode phonon.[21(b)] As various theoretical studies have shown, the clustering phenomenon and the

presence of short-range order should be much more pronounced in the lower-dimensional surface transitions. Therefore, detailed dynamic studies of the surface structural phase transition through inelastic scattering experiments should provide particular interesting results and fruitful comparison with the current theoretical ideas.

ACKNOWLEDGMENT

This work was supported by the National Science Foundation through the Materials Research Laboratory at Brown University.

*Present address.

[1]Experimental studies of surface phase transitions have been recently reviewed; see L. D. Roelofs and P. J. Estrup, Surf. Sci. 125, 51 (1983).

[2]See, for example, T. L. Einstein, in *Chemistry and Physics of Solid Surfaces,* edited by R. Vanselow and R. Howe (Springer, Berlin, 1982), Vol. IV, p. 251.

[3]P. J. Estrup, J. Vac. Sci. Technol. 16, 635 (1979).

[4]G. Gewinner, J. C. Peruchetti, A. Jaegle, and R. Riedinger, Phys. Rev. Lett. 43, 935 (1979).

[5]M. A. Van Hove, R. J. Koestner, P. C. Stair, J. P. Biberian, L. L. Kesmodel, I. Bartos, and G. A. Somorjai, Surf. Sci. 103, 189 (1981); 103, 218 (1981).

[6]N. Osakabe, Y. Tanishiro, K. Yagi, and G. Honjo, Surf. Sci. 109, 353 (1981).

[7]P. A. Bennett and M. B. Webb, Surf. Sci. 104, 74 (1981).

[8]P. W. Davies and R. M. Lambert, Surf. Sci. 107, 391 (1981).

[9]The references bearing on the clean W(100) reconstructive phase transition are far too numerous to cite individually. A recent experimental review is D. A. King, Proceedings of the Nordic Conference on Surface Sciences, August, 1982 [Phys. Scr. T4, 34 (1983)].

[10]T. E. Felter, R. A. Barker, and P. J. Estrup, Phys. Rev. Lett. 38, 1138 (1977).

[11]M. K. Debe and D. A. King, J. Phys. C 10, L303 (1977).

[12]R. A. Barker, P. J. Estrup, F. Jona, and P. M. Marcus, Solid State Commun. 25, 375 (1978).

[13]J. A. Walker, M. K. Debe, and D. A. King, Surf. Sci. 104, 405 (1981).

[14]P. Bak, Phys. Rev. Lett. 44, 889 (1980).

[15]T. Riste, E. J. Samuelson, K. Otnes, and J. Feder, Solid State Commun. 9, 1455 (1971).

[16]S. M. Shapiro, J. D. Axe, G. Shirane, and T. Riste, Phys. Rev. B 6, 4332 (1972).

[17]K. A. Müller and W. Berlinger, Phys. Rev. Lett. 26, 13 (1971).

[18]R. A. Cowley, Philos. Mag. 11, 673 (1964).

[19]J. A. Krumhansl and J. R. Schrieffer, Phys. Rev. B 11, 3535 (1975).

[20]T. Schneider and E. Stoll, Phys. Rev. B 13, 1216 (1976).

[21](a) R. A. Cowley, Adv. Phys. 29, 1 (1980); (b) A. D. Bruce, *ibid.,* 111 (1980); (c) A. D. Bruce and R. A. Cowley, *ibid.,* 219 (1980).

[22]G. Doyen, G. Ertl, and M. Plancher, J. Chem. Phys. 62, 2957 (1975).

[23]P. D. Beale, S. K. Sarker, and J. A. Krumhansl, Phys. Rev. B 24, 266 (1981).

[24]M. E. Fisher and R. J. Burford, Phys. Rev. 156, 583 (1967).

[25]A. J. Melmed, R. T. Tung, W. R. Graham, and G. D. W. Smith, Phys. Rev. Lett. 43, 1521 (1979); R. T. Tung, W. R. Graham, and A. J. Melmed, Surf. Sci. 115, 576 (1982).

[26]P. J. Estrup, L. D. Roelofs, and S. C. Ying, Surf. Sci. 123, L703 (1982); A. J. Melmed and W. R. Graham, *ibid.,* L706 (1982).

[27]D. P. Woodruff, Surf. Sci. (in press).

[28]L. D. Roelofs, G. Y. Hu, and S. C. Ying (unpublished).

[29]D. J. Scalapino, M. Sears, and R. S. Ferrell, Phys. Rev. B 6, 3409 (1975).

[30]A. A. Migdal, Zh. Eksp. Teor. Fiz. 69, 1945 (1975) [Sov. Phys.—JETP 42, 743 (1975)]; L. P. Kadanoff, Ann. Phys. (N.Y.) 100, 359 (1976).

[31]As pointed out by BSK, the transfer-matrix formulation can be easily generalized to other, including nonintegral and even differential, scale factors.

[32]See for example, Lee W. Johnson and R. Dean Riess, *Numerical Analysis* (Addison-Wesley, Reading, Mass., 1977).

[33]The transfer matrix must be diagonalized if nonintegral or in particular differential recursions are sought. This demands a heavy increase in computational effort.

[34]V. J. Emery and R. H. Swendsen, Phys. Lett. 64A, 325 (1977).

[35]S. C. Ying and L. D. Roelofs, Surf. Sci. 125, 218 (1983).

[36]K. Binder, Phys. Rev. Lett. 47, 693 (1981).

[37]T. Schneider and E. Stoll, Phys. Rev. B 13, 1216 (1976).

[38]A. D. Bruce, T. Schneider, and E. Stoll, Phys. Rev. Lett. 43, 1284 (1979).

[39]For a discussion of experimental results on this system, see R. A. Barker and P. J. Estrup, J. Chem. Phys. 74, 1442 (1981), and Ref. 9.

[40]P. Heilmann, K. Heinz, and K. Müller, Surf. Sci. 89, 84 (1979).

[41]R. F. Willis, Surf. Sci. 89, 457 (1979); (private communication).

[42]M. K. Debe and D. A. King, Surf. Sci. 81, 193 (1979).

[43]I. Stensgaard, L. C. Feldman, and P. J. Silverman, Phys. Rev. Lett. 42, 84 (1979).